6564 *Macromolecules* **2009**, *42*, 6564–6571
DOI: 10.1021/ma9012972

Macromolecules
ARTICLE

Bandgap and Molecular Level Control of the Low-Bandgap Polymers Based on 3,6-Dithiophen-2-yl-2,5-dihydropyrrolo[3,4-*c*]pyrrole-1,4-dione toward Highly Efficient Polymer Solar Cells

Lijun Huo,[†] Jianhui Hou,*[,‡] Hsiang-Yu Chen,[†] Shaoqing Zhang,[‡] Yang Jiang,[†] Teresa L. Chen,[†] and Yang Yang*[,†]

[†]*Department of Materials Science and Engineering & California Nanosystems Institute, University of California at Los Angeles, Los Angeles, California 90095, and* [‡]*Solarmer Energy Inc., 3445 Fletcher Avenue, El Monte, California 91731*

Received June 16, 2009; Revised Manuscript Received July 12, 2009

ABSTRACT: A series of low-bandgap polymers based on a soluble chromophore of 3,6-dithiophen-2-yl-2,5-dihydropyrrolo[3,4-*c*]pyrrole-1,4-dione (DPP) unit were synthesized by introducing of different electron-rich building blocks copolymerized with DPP unit. Four new DPP-based polymers, PDPP-DTS, PDPP-F, PDPP-BDT, and PDPP-BDP, were characterized by GPC, TGA, NMR, UV−vis absorption, and electrochemical cyclic voltammetry. The results indicate that their bandgaps as well as their molecular energy levels are readily tuned by copolymerizing with different conjugated electron-donating units. In order to investigate their photovoltaic properties, polymer solar cell (PSC) devices based on PDPP-DTS, PDPP-F, PDPP-BDT, and PDPP-BDP were fabricated with a structure of ITO/PEDOT:PSS/polymers:$PC_{70}BM$(1:2,w/w)/Ca/Al under the illumination of AM 1.5G, 100 mW/cm^2. The power conversion efficiencies (PCE) of the four DPP-based PSC devices were measured and shown in this paper. The best performance of the PSC device was obtained by using PDPP-BDP as the electron donor material, and a PCE of 4.45% with an open-circuit voltage (V_{oc}) of 0.72 V, a short-circuit current (J_{sc}) of 10.0 mA/cm^2, and a fill factor (FF) of 61.8% was achieved, which is the best result among the DPP-based polymer materials. It is apparent that the PDPP-BDP-based device exhibits a very broad response range, covering from 300 to 850 nm. The results of the solar cells indicate that these types of materials are very promising candidates for highly efficient polymer solar cells.

Introduction

The dramatic growing demand for energy throughout the world has placed great emphasis on the exploration of new sources of energy. Solar energy has attracted much interest, as one of the more promising long-term solutions for clean, renewable energy. Compared to commercial inorganic solar cells, polymer solar cells have been developed quite recently, as conducting polymers themselves were discovered in 1977.[1] Several merits of polymer solar cells such as high mechanical flexibility, low fabrication cost, and availability of homogeneous films at large areas have created much research interest, and great efforts have been made to improve the efficiency.[2] So far, bulk-heterojunction solar cells, which are composed of an interpenetrating network of donors and acceptors, have played a leading role in realizing higher efficiencies. Efficiencies up to 4−5% have been achieved from poly(3-hexylthiophene) (P3HT) as the donor and a soluble fullerene derivative, (6,6)-phenyl C_{61}-butyric acid methyl ester (PCBM), as the acceptor.[3] However, further improvement of P3HT-based PSC devices is difficult due to P3HT's intrinsic absorption limit. Therefore, developing low-bandgap photovoltaic materials is an alternative approach for achieving higher efficiency. Recently, some new low-bandgap polymers were reported and exhibited better performance up to 5−6%,[4] which provides a guideline for the material chemists to design and synthesize new polymer materials.

*Corresponding authors: e-mail jhhou@ucla.edu (J.H.), yangy@ucla.edu (Y.Y.).

In order to obtain high-performance photovoltaic polymer materials, it is necessary to design and synthesize conjugated polymers with ideal properties, such as low bandgap, broad absorption range, high mobility, and appropriate molecular energy levels. One potential strategy to make suitable low-bandgap donor materials is to incorporate chromophors highly absorbing in visible and near-infrared regions. As a class of brilliant red high-performance pigments, 3,6-diaryl-2,5-dihydropyrrolo[3,4-*c*]pyrrole-1,4-dione (DPP) has been applied in paints, plastic ink, electroluminescent devices, and transistors.[5,6] The DPP unit has a well-conjugated structure, which leads to strong $\pi-\pi$ interaction,[7] and the lactam part makes the DPP unit exhibit a high electron-withdrawing effect, and hence the DPP unit has high electron affinity.[6b] Therefore, these properties make the DPP unit a potential electron-withdrawing unit in photovoltaic polymer materials, and its recent applications in organic solar cells appear hopeful.[8]

As we know, the required properties of donor materials include not only strong and broad absorption to get good harvesting of sunlight but also proper molecular energy levels to get good charge separation and transportation as well as high open-circuit voltage. Therefore, it is necessary to design and synthesize DPP-based conjugated polymers with ideal properties for realizing high efficiency by copolymerizing with conjugated moieties having different electron-donating properties.

In this work, we selected several typical conjugated building blocks to tune the absorption and molecular energy levels to meet the requirements of an ideal donor toward highly efficient photovoltaic performance. Several commonly used conjugated

 Published on Web 08/06/2009

Scheme 1. Molecular Models of DPP Unit Copolymerized with Different Building Blocks To Tune Bandgap and Molecular Energy Level

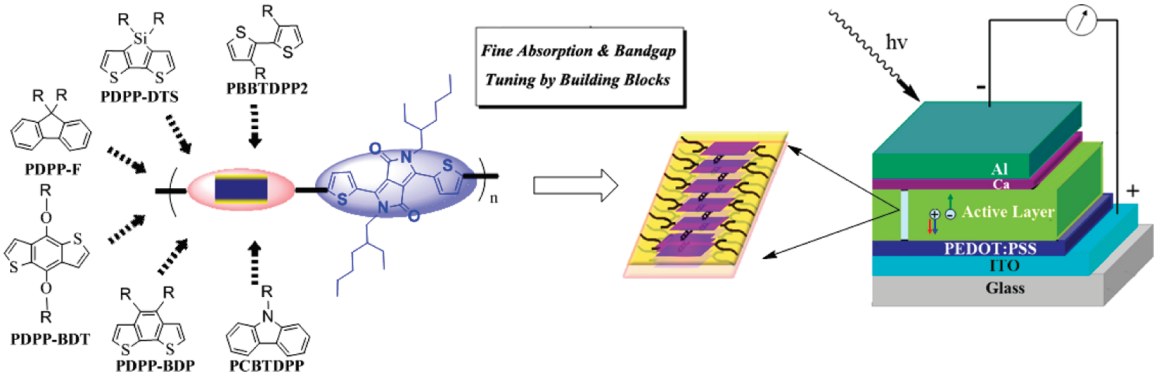

blocks such as dithienosilole, fluorene, benzo[1,2-*b*;3,4-*b*]dithiophene, and benzo[2,1-*b*:3,4-*b*′]dithiophene were copolymerized with DPP units to investigate the relationships between their structures and properties. To get a comprehensive understanding of the properties of DPP-based low-bandgap polymers in polymer solar cells, two other polymers, dithiophene-DPP and carbazole-DPP based polymers, were also discussed in this work.[8]

Experimental Section

Materials. 4,4′-Bis(2-ethylhexyl)-5,5′-dibromodithieno[3,2-*b*:2′,3′-*d*]silole (**3**),[4d] 8-dihydrobenzo[1,2-*b*:4,5-*b*′]dithiophen-4,8-dione (**5**),[9] tetraiodo-2,2′-bithiophene (**7**), and 7-(5,10-diethyl)hexadecyne[10] were prepared according to the published methods. 2-Thiophenecarbonitrile, dimethyl succinate, 2,7-dibromo-9,9-dioctylfluorene, 3-bromothiophene, and $Pd(PPh_3)_4$ were purchased from Sigma-Aldrich Chemical Co., 3-bromothiophene and 2-ethylhexyl bromide were purchased from Acros Chemical Co., and they were used as received. Hexane and tetrahydrofuran (THF) were dried over Na/benzophenone ketyl and freshly distilled prior to use. The other materials were common commercial level and used as received.

Instruments. ^1H and ^{13}C NMR spectra were measured on a Bruker arx-400 spectrometer. Absorption spectra were taken on a Varian Cary 50 ultraviolet−visible spectrometer. The molecular weight of polymers was measured by the GPC method, and polystyrene was used as a standard by using chloroform as eluent. TGA measurement was performed on a Perkin-Elmer TGA-7. The electrochemical cyclic voltammetry was conducted with Pt disk, Pt plate, and Ag/Ag^+ electrode as working electrode, counter electrode, and reference electrode, respectively, in a 0.1 mol/L tetrabutylammonium hexafluorophosphate (Bu_4NPF_6) acetonitrile solution. The polymer films for electrochemical measurements were coated from a polymer−chloroform solution, ca. 5 mg/mL.

Fabrication of Polymer Solar Cells. Polymer solar cell devices with the structure of ITO/PEDOT-PSS/polymers:$PC_{70}BM$ (1:2, w/w)/Ca(10 nm)/Al(80 nm) were fabricated under conditions as follows: After spin-coating a 30 nm layer of poly(3,4-ethylenedioxythiophene):poly(styrenesulfonate) (PEDOT:PSS) onto a precleaned indium−tin oxide (ITO)-coated glass substrates, the polymer/PCBM blend solution was spin-coated. The concentration of the polymer:PCBM blend solution used in this study for spin-coating was 10 mg/mL, and dichlorobenezene was used as the solvent. The thickness of the active layer was ~80 nm. The devices were completed by evaporating Ca/Al metal electrodes with an area of 9.5 mm^2 as defined by masks.

Synthesis. The synthetic routes of the monomers and polymers are shown in Schemes 2 and 3. The detailed synthetic processes are as follows.

3,6-Dithiophen-2-yl-2,5-dihydropyrrolo[3,4-c]pyrrole-1,4-dione (***1***).[8,11] Potassium *tert*-butylate (4 g, 35.7 mmol) was added to a round flask with argon protection. Then a solution of *t*-amyl alcohol (25 mL) and 2-thiophenecarbonitrile (3.27 g, 30 mmol) was injected by a syringe one portion. The mixture was warmed up to 100−110 °C, and a solution of dimethyl succinate (1.46 g, 10 mmol) in *t*-amyl alcohol (8 mL) was dropped slowly in 1 h. When the addition was completed, the reaction was kept at the same temperature for about 1 h, and then the byproduct of methanol was distilled off and the reaction was kept for 2 h. Then the mixture was cooled to 65 °C, diluted with 50 mL of methanol, and neutralized with acetic acid and reflux for another 10 min. Then the suspension is filtered, and the black filter cake is washed by hot methanol and water twice each and dried in vacuum to get coarse product and could be used directly to next step without further purification (2.55 g, yield 85%).

2,5-Diethylhexyl-3,6-dithiophen-2-ylpyrrolo[3,4-c]pyrrole-1,4-dione (***2***). Compound **1** (13.0 g, 43.3 mmol) and anhydrous potassium carbonate (24 g, 173 mmol) were dissolved into *N,N*-dimethylformamide (250 mL) in a two-neck round flask and heated to 145 °C under argon protection. 2-Ethylhexyl bromide (38.6 g, 200 mmol) was injected one portion by syringe. When the reaction was stirred for 15 h at 145 °C, the solution was cooled to room temperature, poured into 500 mL of ice−water, and then filtered. The filter cake was washed by water and methanol several times. After drying in vacuum, the crude product was purified by silica gel chromatography using dichloromethane as eluent to obtain a purple-black solid powder (17.3 g, yield 76%). ^1H NMR ($CDCl_3$, 400 MHz): 8.95 (d, 2H), 7.62 (d, 2H), 7.27 (d, 2H), 4.03 (m, 4H), 1.85 (m, 2H), 1.36−1.22 (m, 16H), 0.85 (m, 12H).

2,5-Diethylhexyl-3,6-bis(5-bromothiophen-2-yl)pyrrolo[3,4-c]-pyrrole-1,4-dione (***M1***). Compound **2** (4.52 g, 8.62 mmol) and *N*-bromosuccinimide (3.14 g, 17.6 mmol) were dissolved into chloroform (200 mL) in a two-neck round flask under argon protection, and then the solution was protected from light and stirred at room temperature. After 40 h, the mixture was poured into 200 mL of methanol and then filtered. The filter cake was washed by hot methanol twice. After drying in vacuum, the pure product was obtained as a purple-black solid (17.3 g, yield 76%). ^1H NMR ($CDCl_3$, 400 MHz): 8.64 (d, 2H), 7.18 (d, 2H), 3.91 (m, 4H), 1.82 (m, 2H), 1.36−1.24 (m, 16H), 0.86 (m, 12H). Calcd for $C_{30}H_{38}N_2O_2S_2Br_2$: C = 52.79; H = 5.61; N = 4.10. Found: C = 52.38; H = 5.59; N = 4.03.

4,4′-Bis(2-ethylhexyl)-5,5′-bis(trimethyltin)dithieno[3,2-b:2′,3′-d]silole (***M2***). Compound **3** (1.2 g, 2.51 mmol) and 20 mL of anhydrous THF were put into a flask and cooled to −78 °C. Subsequently, butyllithium (1.9 mL, 2.9 mol/L in hexane) was added dropwise. After stirring at −78 °C for 30 min, 7 mL of trimethyltin chloride was added in one portion, and then the cooling bath was removed. After the reaction temperature warm up to ambient temperature, the reaction was stirred for another 1 h and then was poured into water and extracted by diethyl ether twice. After removing the solvent, **M2** was obtained as sticky pale green oil (1.78 g, yield 95.6%) and used in the next

Scheme 2. Synthesis Routes of Monomers M1−M5[a]

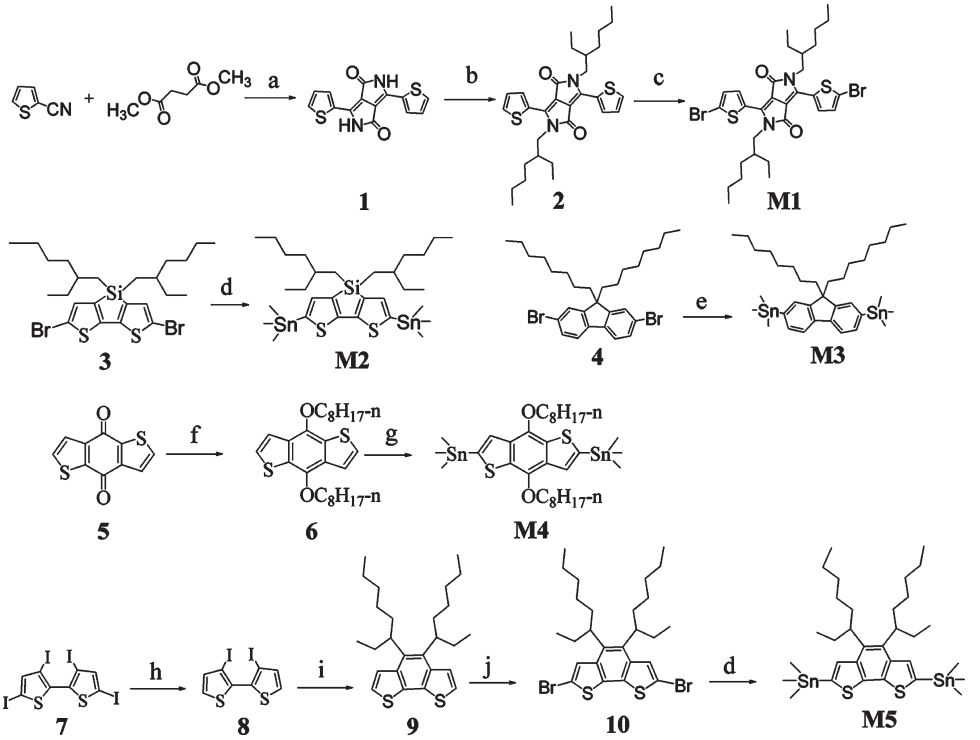

[a] Conditions: (a) *t*-BuOK,*t*-amyl alcohol, 110 °C, 4 h, udner argon; (b) 2-ethyhexyl bromide, DMF, potassium carbonate, 145 °C, 15 h, under argon; (c) NBS, chloroform, rt, 40 h; under argon; (d) butyllithium, −78 °C, 30 min; then trimethyltin chloride, rt, 1 h; (e) butyllithium, THF, −40 °C, 1 h then trimethyltin chloride, rt, 2 h; (f) NaOH, Zn, H_2O, reflux, 1 h, then 1-bromooctane, Bu_4NBr, reflux 12 h; (g) butyllithium, rt, 1 h; then trimethyltin chloride, rt, 2 h; (h) Zn, MeOH, AcOH, 0 °C; (i) dialkyldecyne, $Pd(OAc)_2$, NBu_3, DMF, argon, 130 °C, 12 h; (j) NBS, DMF rt, 15 h.

Scheme 3. Structures and Synthesis of the Polymers by Stille Coupling Reaction

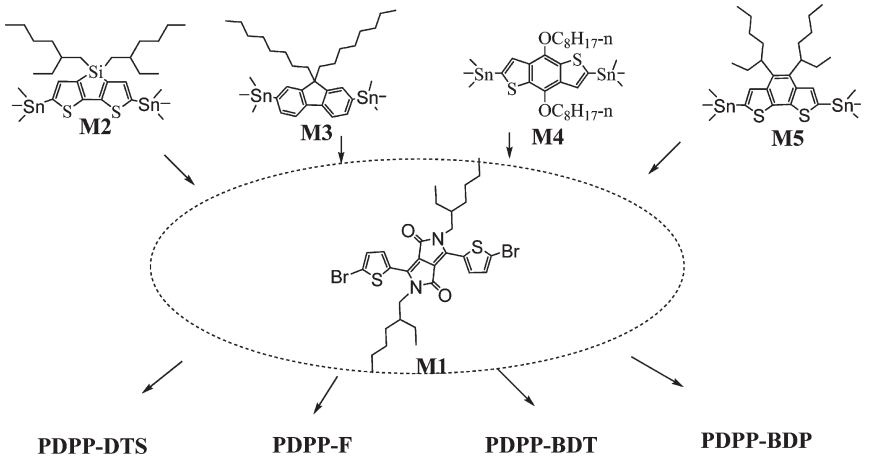

step without any further purification. ^{1}H NMR ($CDCl_3$, 400 MHz), δ (ppm): 7.03(s, 2H), 1.68 (m, 2H), 1.4−1.13 (m, 16H), 0.90 (t, 6H), 0.83 (t, 6H), 0.74 (m, 4H), 0.33 (t, 18H). ^{13}C NMR ($CDCl_3$, 100 MHz), δ (ppm): 154.65, 143.88, 137.91, 137.40, 35.90, 35.60, 28.96, 28.87, 23.02, 17.80, 14.21, 10.85, −8.17. Calcd for $C_{30}H_{54}S_2SiSn_2$: C = 48.41; H = 7.31. Found: C = 48.33; H = 7.30.

2,7- Bis(*trimethyltin*)*-9,9-dioctylfluorene* (***M3***). 2,7-Dibromo-9,9-dioctylfluorene (0.548 g, 1 mmol) and 30 mL of anhydrous THF were put into a flask and cooled to −40 °C . Subsequently, butyllithium (2.4 mmol, 0.82 mL, 2.9 mol/L in hexane) was added dropwise. After stirring at −40 °C for 1 h, 2.6 mL of trimethyltin chloride (1 mol/mL in THF) was added in one portion. Then the cooling bath was removed. After the reaction temperature warmed up to ambient temperature, the reaction was stirred for another 2 h and then was poured into water and extracted by diethyl ether twice. After removing the solvent, **M3** was obtained as a sticky light yellow oil (0.69 g, yield 96.3%) and used in the next step without any further purification. ^{1}H NMR ($CDCl_3$, 400 MHz), δ (ppm): 7.68 (d, 2H), 7.45 (d, 2H), 7.38 (s, 1H), 1.95 (t, 4H), 1.21−0.81 (m, 24H), 0.33 (t, 18H). ^{13}C NMR ($CDCl_3$, 100 MHz), δ (ppm): 150.12, 141.28, 140.84, 133.91, 130.20, 119.19, 54.95, 39.99, 31.80, 29.92, 29.17, 29.08, 23.75, 22.64, 14.10, −9.29. Calcd for $C_{35}H_{58}Sn_2$: C = 58.69; H = 8.16. Found: C = 58.57; H = 8.06.

4,8-Dioctyloxybenzo[*1,2-b;3,4-b*]*dithiophene* (***6***). Compound **5** (8.8 g, 40 mmol), zinc powder (5.72 g, 88 mmol), and 100 mL of water were put into a 250 mL flask; then 24 g of NaOH was added into the mixture. The mixture was well stirred and heated to reflux for 1 h. During the reaction, the color of the

mixture changed from yellow to red and then to orange. Then, 1-bromooctane (23.16 g, 120 mmol) and a catalytic amount of tetrabutylammonium bromide were added into the flask, and the reaction mixture was refluxed for 12 h. The reaction mixture was poured into cold water and extracted by diethyl ether two times. The ether layer was dried over anhydrous $MgSO_4$. After removing solvent, the crude product was purified by recrystallization from ethyl alcohol to get compound **6** (27.28 g, yield 77%) as a colorless crystal. GC-MS: m/z = 446. ^{1}H NMR ($CDCl_3$, 400 MHz), δ (ppm): 7.66 (d, 2H), 7.47 (d, 2H), 4.26 (t, 4H), 1.87 (quintuple, 4H), 1.53 (m, 4H), 1.37−1.27 (m, 32H), 0.88 (t, 6H).

2,6-Bis(trimethyltin)-4,8-dioctyloxybenzo[1,2-b;3,4-b]dithiophene (***M4***). Compound **6** (4.30 g, 6 mmol) and 100 mL of THF were added into a flask under an inert atmosphere. *n*-Butyllithium (13.2 mmol, 2.9 M in *n*-hexane) was added dropwise into the solution at rt, and after being stirred for 1 h at rt, a great deal of white solid precipitate appeared in the flask. Then, 14 mmol of trimethyltin chloride (14 mL, 1 M in *n*-hexane) was added in one portion, and the reactant turned clear rapidly. The cooling bath was removed, and the reaction was stirred at ambient temperature for 2 h. Then, it was poured into 200 mL of cool water and extracted by ether three times. The organic layer was washed with water two times and then dried by anhydrous $MgSO_4$. After removing solvent under vacuum, the residue was recrystallized from ethyl alcohol two times. 4.03 g of compound **M4** was obtained as colorless needle crystals (3.3 g, yield 71%). ^{1}H NMR ($CDCl_3$, 400 MHz), δ (ppm): 7.62 (s, 2H), 4.15 (t, 4H), 1.79 (quintuple, 4H), 1.53 (m, 4H), 1.33−1.28 (m, 32H), 0.87 (t, 6H). ^{13}C NMR ($CDCl_3$, 100 MHz), δ (ppm): 143.15, 140.49, 134.09, 133.01, 129.10, 128.04, 73.63, 31.97, 30.58, 29.76, 29.71, 29.55, 29.40, 26.16, 22.73, 14.16, −8.31. Calcd for $C_{32}H_{54}O_2S_2Sn_2$: C = 49.76; H = 7.05. Found: C = 49.34; H = 6.99.

3,3′-Diiodo-2,2′-bithiophene (***8***). Compound **7**, 3,3′,5,5′-tetraiodo-2,2′-bithiophene (34.4 g, 51 mmol), and zinc powder (8.6 g, 132 mmol) were added into the mixture of methanol (350 mL) and acetate acid (14 mL) in portions at 0 °C and stirred for 50 min at 0 °C. Then the mixture was filtered, and the filter cake was washed with methanol several times. The filtrate was collected, the solvent was removed, and the residue was recrystallized from methanol to get white powder (9.8 g, yield 45%). GC-Ms: m/z = 418. ^{1}H NMR (δ/ppm, $CDCl_3$, 400 MHz): 7.42 (d, 2H), 7.17 (d, 2H).

4,5-Bis(2-ethylhexyl)benzo[2,1-b:3,4-b′]dithiophene (***9***). 3,3′-Diiodo-2,2′-bithiophene (1.0 g, 2.4 mmol) and 7-(5,10-diethyl)-hexadecyne (1.8 g, 7.2 mmol) and $Pd(OAc)_2$ (54 mg, 0.24 mmol) were added into a flask under argon protection. Then tributylamine (1.3 g, 7.2 mmol) and anhydrous DMF (10 mL) were added and warmed to 130 °C. After 12 h the reaction was cooled to room temperature and poured into water and extracted by ethyl ether; the solvent was removed, and the residue was purified by column chromatography on silica gel with hexane as eluent to get a colorless sticky liquid (0.47 g, yield: 47%). GC-Ms: m/z = 414. ^{1}H NMR (δ/ppm, $CDCl_3$, 400 MHz): 7.46 (d, 2H), 7.33 (d, 2H), 3.03 (m, 4H), 1.75−1.33 (m, 18H), 0.84 (t, 12H). ^{13}C NMR ($CDCl_3$, 100 MHz), δ (ppm): δ 137.94, 131.75, 131.36, 124.27, 123.05, 41.51, 35.01, 32.85, 29.15, 26.09, 23.23, 14.18, 11.37.

2,7-Dibromo-4,5-bis(2-ethylhexyl)benzo[2,1-b:3,4-b′]dithiophene (***10***). NBS (0.90 g, 5.07 mmol) was added into a solution of 4,5-diethylhexylbenzo[2,1-*b*:3,4-*b*′]dithiophene (0.7 g, 1.69 mmol) in DMF (20 mL) by portions at room temperature. After 15 h, the mixture was washed by water, extracted by ethyl ether, and further purified by column chromatography on silica gel with hexane as eluent to get a colorless stick liquid. White solid (0.78 g, yield: 80%) GC-MS: m/z = 572. ^{1}H NMR (δ/ppm, $CDCl_3$, 400 MHz): 7.49 (s, 2H), 3.07(m, 4H), 1.79−1.41 (m, 18H), 0.99 (t, 12H). ^{13}C NMR ($CDCl_3$, 100 MHz), δ (ppm): 137.67, 131.49, 131.22, 126.79, 112.34, 41.36, 34.92, 32.61, 29.02, 25.82, 23.08, 14.16, 11.32.

2,7-Bis(trimethyltin)-4,5-bis(2-ethylhexyl)benzo[2,1-b:3,4-b′]dithiophene (***M5***). 2,7-Dibromo-4,5-bis(2-ethylhexyl)benzo-[2,1-*b*:3,4-*b*′]dithiophene (0.43 g, 0.75 mmol) and 20 mL of anhydrous THF were put into a flask and cooled to −78 °C. Subsequently, butyllithium (0.60 mL, 2.9 mol/L in hexane) was added dropwise. After stirring at −78 °C for 30 min, trimethyltin chloride (2 mL, 1 M) was added in one portion, and then the cooling bath was removed. After the reaction temperature warmed to ambient temperature, the reaction was stirred for another 1 h and then was poured into water and extracted by diethyl ether twice. After removing solvent, **M5** was obtained as light yellow oil (0.54 g, yield 97.3%) and used in the next step without any further purification. ^{1}H NMR ($CDCl_3$, 400 MHz), δ (ppm): 7.52 (s, 2H), 3.03 (m, 4H), 1.71−1.34 (m, 18H), 0.90 (t, 12H), 0.36 (t, 18H). ^{13}C NMR ($CDCl_3$, 100 MHz), δ (ppm): 138.43, 137.07, 135.88, 131.34, 130.92, 40.27, 35.81, 32.52, 28.96, 25.77, 23.09, 14.13, 11.01, −8.08. Calcd for $C_{32}H_{54}S_2Sn_2$: C = 51.92; H = 7.35. Found: C = 51.84; H = 7.31.

General Synthetic Procedure of PDPP-DTS, PDPP-F, PDPP-BDT, and PDPP-BDP by Stille Reaction. The polymers were prepared by a similar procedure of coupling 2,5-diethylhexyl-3,6-bis(5-bromothiophene-2-yl)pyrrolo[3,4-*c*]pyrrole-1,4-dione. **M1** and monomers of **M2**, **M3**, **M4**, and **M5**, respectively. 1.0 mmol of the monomer was put into a three-neck flask. Then 15 mL of degassed toluene and 1.0 mmol of **M1** were added under the protection of argon. The solution was flushed with argon for 10 min, and then 30 mg of $Pd(PPh_3)_4$ was added. After another flushing with argon for 20 min, the reactant was heated to reflux for 18 h. Then the reactant was cooled to room temperature, and the polymer was precipitated by adding 50 mL of methanol, filtered through a Soxhlet thimble, and then subjected to Soxhlet extraction with methanol, hexane, and chloroform. The polymer was recovered as solid from the chloroform fraction by rotary evaporation. The solid was dried under vacuum for 1 day. The yield, ^{1}H NMR, and molecular weight of polymers are as follows:

Poly{4,4′-bis(2-ethylhexyl)dithieno[3,2-b:2′,3′-d]silole-alt-5-diethylhexyl-3,6-bis(5-bromothiophen-2-yl)pyrrolo[3,4-c]pyrrole-1,4-dione}, PDPP-DTS. Yield: 29%. ^{1}H NMR (400 MHz, $CDCl_3$): 8.94 (br, 2H), 7.52−6.68 (br, 4H), 4.24 (br, 4H), 1.85 (br, 4H), 1.67−0.84 (m, 60H). M_n = 11.1K; polydispersity = 2.8.

Poly{2,7′-9,9-dioctylfluorene-alt-5-diethylhexyl-3,6-bis(5-bromothiophen-2-yl)pyrrolo[3,4-c]pyrrole-1,4-dione}, PDPP-F. Yield: 52%. ^{1}H NMR (400 MHz, $CDCl_3$): 8.91 (br, 2H), 7.79−7.36 (m, 8H), 4.38 (br, 4H), 1.94 (br, 4H), 1.67−0.77 (m, 60H). M_n = 11.6K; polydispersity = 1.6.

Poly{2,6′-4,8-dioctyloxybenzo[1,2-b;3,4-b]dithiophene-alt-5-diethylhexyl-3,6-bis(5-bromothiophen-2-yl)pyrrolo[3,4-c]pyrrole-1,4-dione}, PDPP-BDT. Yield: 41%. ^{1}H NMR (400 MHz, $CDCl_3$): 8.96 (br, 2H), 7.69−6.99 (br, 4H), 4.24−3.73 (br, 8H), 2.07−0.74 (m, 60H). M_n = 8.5K; polydispersity = 2.4.

Poly{2,7′-4,5-bis(2-ethylhexyl)benzo[2,1-b:3,4-b′]dithiophene-alt-5-diethylhexyl-3,6-bis(5-bromothiophen-2-yl)pyrrolo[3,4-c]-pyrrole-1,4-dione}, PDPP-BDP. Yield: 41%. ^{1}H NMR (400 MHz, $CDCl_3$): 8.90 (br, 2H), 7.67−6.76 (br, 4H), 4.25 (br, 4H), 3.01 (br, 4H), 2.04−0.81 (m, 60H). M_n = 22.7K; polydispersity = 2.1.

Results and Discussion

Synthesis and Structural Characterization. The general synthetic strategy for the monomers and polymers is outlined in Scheme 3. In order to keep good solubility of the DPP derivative **M1**, 2-ethylhexyl chains were added to the lactam NH groups. **M2** and **M4** were synthesized by the reported methods.[4d,9] Compound **8** was synthesized by zinc power reduction reaction on tetraiodobithiophene, compound **7**, at 0 °C in acid conditions. By Stille coupling reaction in toluene

using $Pd(PPh_3)_4$ as catalyst at 110 °C for 18 h, the polymers PDPP-DTS, PDPP-F, PDPP-BDT, and PDPP-BDP were obtained with a yield of 40−60%. All the polymers are soluble in chloroform ($CHCl_3$), chlorobenzene, and dichlorobenznene. The weight-average molecular weights (M_w) of PDPP-DTS, PDPP-F, PDPP-BDT, and PDPP-BDP were determined by gel permeation chromatography (GPC) against polystyrene standards in $CHCl_3$ eluent, and the detailed GPC data are listed in Table 1.

The ^{1}H NMR spectra of the polymers are shown in Figure 1. All spectra show signals of the DPP thienoyl protons at about 8.9 ppm and signals of the ethylhexyl-substituted lactam groups of DPP in the region from 0.7 to 1.8 ppm. The signal of the methylene group adjacent to the lactam N atom appears around 4.2 ppm. In all polymers, for every conjugated subunit such as dithienosilole, fluorene, benzo[1,2-*b*;3,4-*b*]dithiophene, and benzo[2,1-*b*:3,4-*b*′]dithiophene, their aromatic protons showed broader resonance peaks ranging from 6.7 to 7.8 ppm due to the polymeric characters. The resonance peaks of the methylene protons (marked e positions in Figure 1) of the ethylhexyl- or octyl-substituted side chains appear at 1.8, 1.9, 3.9, and 3.0 ppm.

Thermal Stability. Thermal stability of the polymers was investigated with thermogravimetric analysis (TGA), as shown in Figure 2. The TGA analysis reveals that, in the air, the onset points of the weight loss with 5% weight-loss temperature (T_d) of PDPP-DTS, PDPP-F, PDPP-BDT, and PDPP-BDP are 344, 349, 319, and 352 °C. This indicates that all of them have good thermal stability against oxygen, which is very important in device fabrication process and other kinds of applications.

Optical Properties. The photophysical characteristics of the polymers were investigated by ultraviolet−visible (UV−vis) absorption spectroscopy in dilute chloroform solutions and as spin-coated films on quartz substrates. Figure 3a shows the absorption spectra of the PDPP-DTS, PDPP-F, PDPP-BDT, and PDPP-BDP in chloroform, and the optical data including the absorption peak wavelength ($\lambda_{max,abs}$), absorption edge wavelength ($\lambda_{edge,abs}$) in both solutions and films, and the optical band gap (E_g^{opt}) are summarized in Table 2. It can be seen from Figure 3a that all the absorption spectra in dilute chloroform appear as two absorption bands. All of the polymers have an absorption band located at 300−500 nm, and the second broad absorption band from 500 to 900 nm in long wavelength region should correspond to the $\pi-\pi^*$ transition of the conjugated polymer main chains. Absorption spectra of these four polymers appear as near-infrared absorption, and the peaks are located at 798, 649, 750, and 727 nm for PDPP-DTS, PDPP-F, PDPP-BDT, and PDPP-BDP, respectively. It was found that all four polymers in long wavelength regions exhibited shoulder peaks, which are related not only to the intermolecular aggregation state caused by the strong polarity of the lactam groups of DPP units[7] but also to the increased vibronic coupling associated with molecular rigidity imposed by molecular connectivity in solution measurements. From Figure 3b it can be seen that these four polymers show extended absorption edges in films in the NIR region, which can be attributed to the more aggregated configuration formed in solid state. The absorption edges are listed in Table 2, corresponding to the optical bandgaps

Table 1. Molecular Weights and Thermal Properties of the Polymers

polymer	M_w[a]	M_n[a]	PDI[a] (M_w/M_n)	T_d[b] (°C)
PDPP-DTS	31.1K	11.1K	2.8	344
PDPP-F	18.6K	11.6K	1.6	349
PDPP-BDT	20.4K	8.5K	2.4	319
PDPP-BDP	47.7K	22.7K	2.1	352

[a] M_n, M_w, and PDI of the polymers were determined by gel permeation chromatography using polystyrene standards in $CHCl_3$. [b] The 5% weight-loss temperatures in the air.

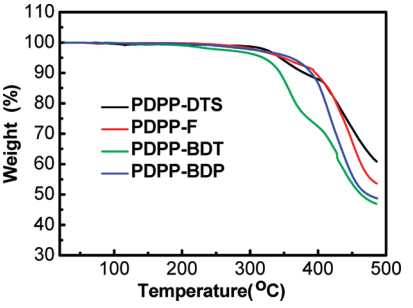

Figure 2. TGA plots of the polymers with a heating rate of 10 °C/min in the air.

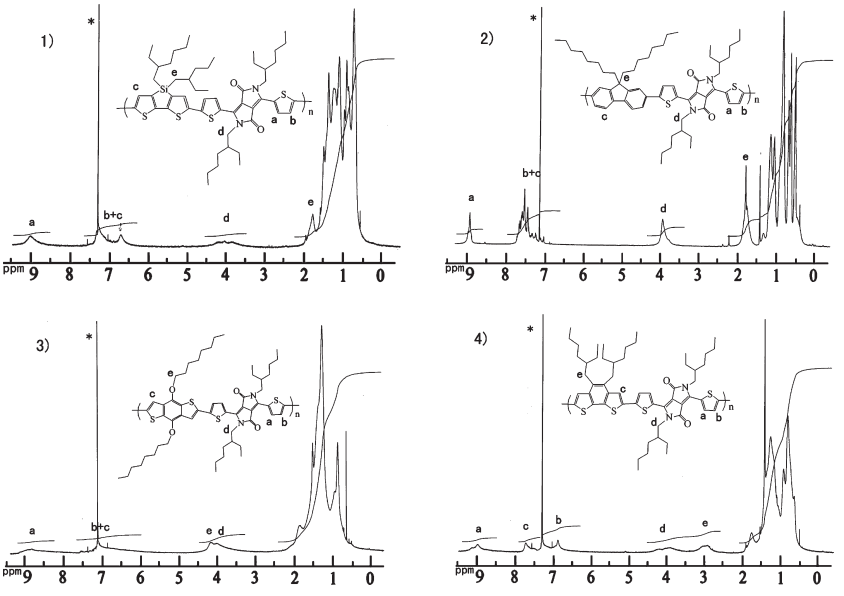

Figure 1. ^{1}H NMR spectrum of the polymers (1) PDPP-DTS, (2) PDPP-F, (3) PDPP-BDT, and (4) PDPP-BDP.

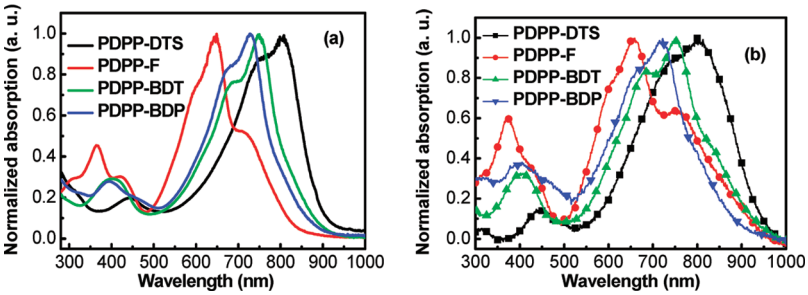

Figure 3. Normalized UV−vis−NIR absorption spectra of PDPP-DTS, PDPP-F, PDPP-BDT, and PDPP-BDP in (a) dilute $CHCl_3$ solutions and (b) thin films on a quartz plate.

Table 2. Optical Properties of PDPP-DTS, PDPP-F, PDPP-BDP, and PDPP-BDP

	$\lambda_{max,abs}$ (nm)		λ_{onset} (nm)	
	solution	film	film	E_g^{opt} (eV)[c]
PDPP-DTS	798	796	963	1.29
PDPP-F	649	652	945	1.31
PDPP-BDT	750	750	942	1.31
PDPP-BDP	727	722	928	1.34
PBBTDPP2[a]	650		886	1.40
PCBTDPP[b]	642	680	792	1.57

[a] Reference 8a. [b] Reference 8e. [c] Calculated from the absorption band edge of the copolymer films, $E_g = 1240/\lambda_{edge}$.

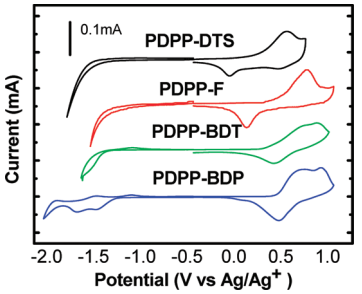

Figure 4. Cyclic voltammograms of PDPP-DTS, PDPP-F, PDPP-BDT, and PDPP-BDP films on platinum electrode in acetonitrile solution containing 0.1 mol/L Bu_4NPF_6 at a scan rate of 20 mV/s.

(E_g^{opt}) of 1.29, 1.31, 1.31, and 1.34 eV for PDPP-DTS, PDPP-F, PDPP-BDT, and PDPP-BDP, respectively.

Electrochemical Properties. Electrochemical cyclic voltammetry has been widely employed to investigate the redox behavior of the polymer and to estimate its HOMO and LUMO energy levels.[12] Figure 4 shows the cyclic voltammograms of PDPP-DTS, PDPP-F, PDPP-BDT, and PDPP-BDP films on a Pt electrode in a 0.1 mol/L Bu_4NPF_6−acetonitrile solution. The results of the electrochemical measurements are listed in Table 3. It can be seen from Figure 4 that there are irreversible n-doping/dedoping (reduction/reoxidation) processes in the negative potential range for all the polymers. However, there is reversible p-doping/dedoping (oxidation/rereduction) process in the positive potential range for PDPP-DTS, PDPP-F, PDPP-BDT, and PDPP-BDP. The onset oxidation potential (E_{ox}) is 0.34 V vs Ag/Ag^+ for PDPP-DTS, 0.53 V for PDPP-F, 0.46 V for PDPP-BDT, and 0.51 V for PDPP-BDP. Among the four polymers, PDPP-DTS possesses the lowest onset oxidation potential of 0.34 V, indicating that the electron-donating ability of dithienosilole is the strongest among these four electron-donating units. From the electrochemical oxidation doping results we can conclude that the oxidation potentials

Table 3. Electrochemical Properties of PDPP-DTS, PDPP-F, PDPP-BDT, and PDPP-BDP

	E_{onset}^{ox} (V)	E_{onset}^{red} (V)	HOMO (eV)	LUMO (eV)	E_g^{ec} (eV)[c]	E_g^{opt} (eV)
PDPP-DTS	0.34	−1.23	−5.04	−3.47	1.57	1.29
PDPP-F	0.53	−1.10	−5.23	−3.60	1.63	1.31
PDPP-BDT	0.46	−1.19	−5.16	−3.51	1.65	1.31
PDPP-BDP	0.51	−1.07	−5.21	−3.63	1.58	1.34
PBBTDPP2[a]	0.3	−1.4			1.70	1.40
PCBTDPP[b]	0.74	−0.78	−5.44	−3.92	1.52	1.57

[a] Reference 8a. [b] Reference 8e. [c] Calculated from $E_g = e(E_{onset}^{ox} - E_{onset}^{red})$.

of the polymers of PDPP-DTS, PDPP-F, PDPP-BDT, and PDPP-BDP are proportional to their corresponding electron-donating abilities of dithienosilole, fluorene, benzo[1,2-*b*;3,4-*b*]dithiophene, and benzo[2,1-*b*:3,4-*b*′]dithiophene, which also coincide with their optical absorption properties. In the reductive potential region, the onset reduction potential (E_{red}) is −1.23 V vs Ag/Ag^+ for PDPP-DTS, −1.10 V for PDPP-F, −1.19 V for PDPP-BDT, and −1.07 V for PDPP-BDP.

From the onset oxidation potentials (E_{onset}^{ox}) and the onset reduction potentials (E_{onset}^{red}) of the polymers, HOMO and LUMO energy levels as well as the energy gap of the polymers were calculated according to the equations LUMO = $-e(E_{red} + 4.7)$ (eV) and HOMO = $-e(E_{ox} + 4.7)$ (eV), where the units of E_{ox} and E_{red} are V vs Ag/Ag^+. The E_{LUMO} and the E_{HOMO} values of the polymers are included in Table 3. Table 3 shows that the HOMO energy level of PDPP-F has the lowest value of −5.23 eV and that of PDPP-DTS has the highest value of −5.04 eV and PDPP-BDT and PBDPDPP appear to have middle values of −5.16 and −5.21 eV, respectively. Correspondingly, the LUMO energy level of PDPP-DTS, PDPP-F, PDPP-BDT, and PDPP-BDP are −3.47, −3.60, −3.51, and −3.63 eV, respectively. The electrochemical bandgap, E_g^{ec}, calculated from $E_g^{ec} = e(E_{onset}^{ox} - E_{onset}^{red})$, are 1.57, 1.63, 1.65, and 1.58 eV for PDPP-DTS, PDPP-F, PDPP-BDT, and PDPP-BDP, respectively.

In order to make a clear comparison, properties of two other DPP-based polymers, PBBTDPP2 and PCBTDPP, have also been listed in Table 3 according to the reported works.[8a,8e] The results indicate that the bandgap as well as the molecular energy level of DPP-based polymers can be adjusted by copolymerizing with different electron-donating groups. When the electron-donating unit was replaced by carbazole, the HOMO energy level even reached −5.44 eV. The LUMO levels of these polymers also vary from −3.47 to −3.92 eV.

Photovoltaic Properties. The bulk heterojunction polymer solar cells (PSCs) were fabricated with a structure of ITO/PEDOT:PSS/polymers: $PC_{70}BM$ (1:2 wt %)/Ca/Al,

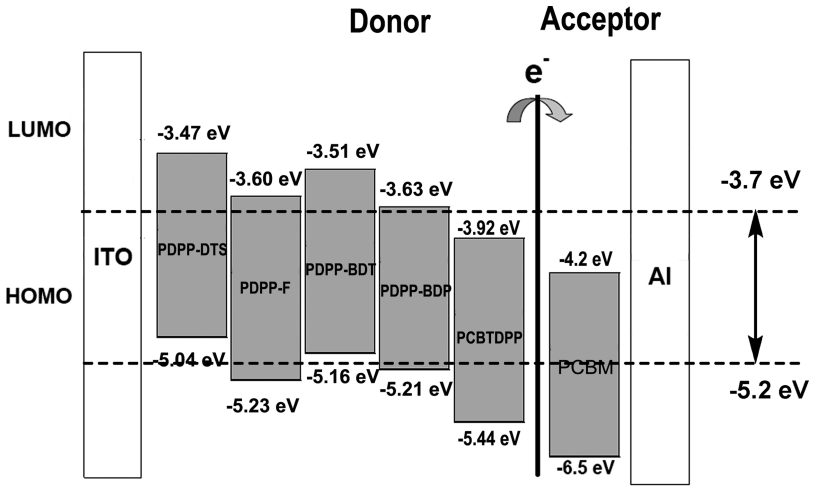

Figure 5. Energy level diagrams for PDPP-DTS, PDPP-F, PDPP-BDT, and PDPP-BDP.

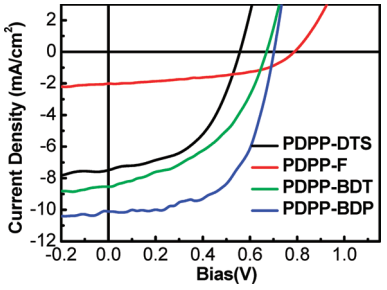

Figure 6. $I-V$ curves of the PSCs based on PDPP-DTS, PDPP-F, PDPP-BDT, and PDPP-BDP under illumination of AM1.5G, 100 mW/cm^2.

Table 4. Photovoltaic Properties of the PSCs Based on the DPP-Based Polymers

polymer:P_{70}CBM (1:2)	V_{oc} (V)	J_{sc} (mA/cm^2)	FF (%)	PCE (%)
PDPP-DTS	0.55	7.5	50.8	2.10
PDPP-F	0.78	2.0	49.9	0.78
PDPP-BDT	0.68	8.4	44.3	2.53
PDPP-BDP	0.68	10.1	62.7	4.31
PDPP-BDP[a]	0.72	10.0	61.8	4.45
PBBTDPP2	0.66	9.4	47.0	2.9
PCBTDPP[b]	0.85	5.2	37.0	1.6

[a] Annealed at 110 °C for 30 min. [b] $PC_{60}BM$.

where the polymers were used as electron donors and $PC_{70}BM$ was used as electron acceptor. Figure 6 shows $I-V$ curves of the devices, and Table 4 lists the corresponding V_{oc}, J_{sc}, FF, and PCE of the devices under the illumination of AM 1.5G, 100 mW/cm^2.

Figure 6 shows the $I-V$ curves of the devices, and V_{oc}, J_{sc}, FF, and PCE data were collected and listed in Table 4. It is very clear that the PSC devices based on these four DPP-based polymers exhibit different open-circuit voltages, which are consistent with their HOMO levels. For example, PDPP-DTS exhibits a HOMO level of −5.04 eV, which is the highest value among these four materials; as a result, the open-circuit voltage obtained by PDPP-DTS was the lowest at only 0.55 V; accordingly, the highest V_{oc} of these four materials was obtained from PDPP-F, the polymer having the lowest HOMO level.

As reported, the photovoltaic properties of conjugated polymers are very susceptible to molecular structure. Even for the conjugated polymers with identical conjugated main

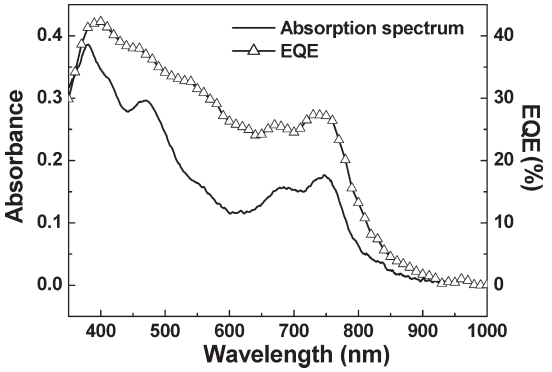

Figure 7. Absorption spectrum and EQE curves of the PSCs based on PDPP-BDP:$PC_{70}BM$ (1:2, w/w) annealed under 110 °C for 30 min.

chains, their photovoltaic properties vary with their side chains. For example, the number of carbons in the alkyl side chain of polythiophene can greatly affect the hole mobility of poly(3-alkylthiophene)[13] as well as its photovoltaic properties,[14] and the PCE of poly(3-hexylthiophene):PCBM-based solar cell is about ∼10 times higher than that of the poly(3-butylthiophene):PCBM-based device. Therefore, it is hard to reach a solid conclusion by comparison of the parameters, including FF, J_{sc}, and hence PCE, of the devices based on these four DPP-based polymers.

It is worthy to mention that another DPP-based polymer, PBBTDPP2, exhibited some interesting photovoltaic properties in PSC devices. As reported, by using pure dichlorobenzene as solvent during the spin-coating process, the PCE of the device was 2.9%; however, PCE of the PDPP-BDP-based PSC device can be improved to 4.0% by using a mixed solvent of chloroform and dichlorobenzene. Since the polymer PDPP-BDP exhibited the highest PCE value in these four materials, it was selected to improve photovoltaic properties by using another different treatment during the device fabrication process. In this work, the annealing process in the glovebox was used to improve photovoltaic properties of the PDPP-BDP-based devices. We tried different annealing conditions of the device, and it was found that the best performance was obtained when the device was annealed under 110 °C for 30 min. As shown in Table 4, after annealing, the J_{sc} and the FF of the device decreased slightly, but the V_{oc} increased from 0.68 to 0.72 V, and as a result, the PCE was improved to 4.45% from 4.31%.

This result indicates that annealing is not an effective approach to improve performance of PDPP-BDP-based devices, and further optimizations are in progress.

The absorption spectrum of the PDPP-BDP:$PC_{70}BM$ blend film prepared under the same conditions as those described in the device fabrication section is shown in Figure 7. The EQE curve of the PSC device is also plotted in Figure 7 for comparison. It is apparent that the device exhibits a very broad response range, covering from 300 to 850 nm, but the external quantum efficiency (EQE) of the device is within 40% for almost the whole absorption range. The main reason for the low EQE of the device is due to the limited absorbance value of the active layer; as shown in Figure 7, it is known that the absorption in the long wavelength region is contributed by the polymer, and the absorption in the short wavelength region is mainly from $PC_{70}BM$; however, the peak value of the absorbance in the long wavelength region is only ~0.18, which means that only a small part of sunlight is absorbed in the device. As reported, the EQE of P3HT:PCBM or some of other low-bandgap polymer-based PSCs can exceed 60% or even 70%. Therefore, if the EQE of the device can be improved by increasing the thickness of the active layer without hampering charge separation and transport properties, the device performance can be improved significantly. Additionally, a ~5% difference between the J_{sc} and the integral of the EQE by the solar irritation spectrum, AM 1.5G, 100 mW, is observed, which provides good proof of the reliability for the photovoltaic results.

Conclusions

To improve the high efficiency of polymer solar cells, a soluble chromophore of 3,6-dithiophen-2-yl-2,5-dihydropyrrolo[3,4-*c*]pyrrole-1,4-dione (DPP) was copolymerized with different electron-rich building blocks such as dithienosilole, fluorene, benzo[1,2-*b*;3,4-*b*]dithiophene, and benzo[2,1-*b*:3,4-*b*′]dithiophene to yield the polymers of PDPP-DTS, PDPP-F, PDPP-BDT, and PDPP-BDP. UV−vis absorption spectra revealed that the electron-donating ability decreases in the order of dithienosilole, benzo[1,2-*b*;3,4-*b*]dithiophene, benzo[2,1-*b*:3,4-*b*′]dithiophene, and fluorene, which coincides with their electrochemical data. By fine-tuning the bandgap and molecular level of DPP-based polymers, proper electrochemical energy levels (HOMO and LUMO) and a lower bandgap of ~1.3 eV were realized. The PSCs based on PDTSDPP, PFDPP, PBDTDPP, and PBDPDPP were fabricated with a structure of ITO/PEDOT:PSS/polymers:$PC_{70}BM$ (1:2 wt %)/Ca/Al under the illumination of AM 1.5G, 100 mW/cm^2. The photovoltaic performances of these polymers varied obviously due to different building blocks copolymerized in DPP-based polymers main chains. The best performance of the PSC device was obtained by using PDPP-BDP as the electron donor material, and a PCE of 4.45% with an open-circuit voltage (V_{oc}) of 0.72 V, a short-circuit current (J_{sc}) of 10.0 mA/cm^2, and a fill factor (FF) of 61.8% was achieved, which is the best result thus far for DPP-based polymer materials. It is apparent that the PDPP-BDP-based device exhibit very broad response range, covering from 300 to 850 nm. The results of the solar cells indicate that these kinds of materials are very promising candidates for highly efficient polymer solar cells.

Acknowledgment. This work was financially supported by Solarmer Energy Inc., UC Discovery Grant (Grant GCP05-10208). We thank Miss Huai-Hsuan Tsai for the initial photovoltaic testing of one of the materials.

References and Notes

(1) Shirakawa, H.; Louis, J.; MacDiarmid, A. G.; Chiang, C. K.; Heeger, A. J. *Chem. Commun*. **1977**, *16*, 578.
(2) (a) Sariciftci, N. S.; Braun, D.; Zhang, C.; Srdanov, V.; Heeger, A. J.; Stucky, G.; Wudl, F. *Appl. Phys. Lett*. **1993**, *62*, 585. (b) Yu, G.; Gao, J.; Hummelen, J. C.; Wudl, F.; Heeger, A. J. *Science* **1995**, *270*, 1789. (c) Huynh, W. U.; Dittmer, J. J.; Alivisatos, A. P. *Science* **2002**, *295*, 2425. (d) Coakley, K. M.; McGehee, M. D. *Chem. Mater*. **2004**, *16*, 4533.
(3) (a) Li, G.; Shrotriya, V.; Huang, J. S.; Yao, Y.; Moriarty, T.; Emery, K.; Yang, Y. *Nat. Mater*. **2005**, *4*, 864. (b) Ma, W. L.; Yang, C. Y.; Gong, X.; Lee, K. H.; Heeger, A. J. *Adv. Funct. Mater*. **2005**, *15*, 1617. (c) Li, G.; Shrotriya, V.; Yao, Y.; Yang, Y. *J. Appl. Phys*. **2005**, *98*, 043704.
(4) (a) Muhlbacher, D.; Scharber, M.; Morana, M.; Zhu, Z. G.; Waller, D.; Gaudiana, R.; Brabec, C. *Adv. Mater*. **2006**, *18*, 2884. (b) Peet, J.; Kim, J. Y.; Coates, N. E.; Ma, W. L.; Moses, D.; Heeger, A. J.; Bazan, G. C. *Nat. Mater*. **2007**, *6*, 497. (c) Wang, E. G.; Wang, L.; Lan, L. F.; Luo, C.; Zhuang, W. L.; Peng, J. B.; Cao, Y. *Appl. Phys. Lett*. **2008**, *92*, 33307. (d) Hou, J. H.; Chen, H. Y.; Zhang, S. Q.; Li, G.; Yang, Y. *J. Am. Chem. Soc*. **2008**, *130*, 16144. (e) Liang, Y. Y.; Wu, Y.; Feng, D. Q.; Tsai, S. T.; Son, H. J.; Li, G.; Yu, L. P. *J. Am. Chem. Soc*. **2009**, *131*, 56. (f) Liang, Y. Y.; Feng, D. Q.; Wu, Y.; Tsai, S. T.; Li, G.; Ray, C.; Yu, L. P. *J. Am. Chem. Soc*. **2009**, *131*, 7792. (g) Park, S. H.; Roy, A.; Beaupre, S.; Cho, S.; Coates, N.; Moon, J. S.; Moses, D.; Leclerc, M.; Lee, K.; Heeger, A. J. *Nat. Photonics* **2009**, *3*, 297–303.
(5) Hao, Z.; Iqbal, A. *Chem. Soc. Rev*. **1997**, *26*, 203.
(6) (a) Beyerlein, T.; Tieke, B. *Macromol. Rapid Commun*. **2000**, *21*, 182. (b) Cao, D.; Liu, Q.; Zeng, W.; Han, S.; Peng, J.; Liu, S. *J. Polym. Sci., Part A: Polym. Chem*. **2006**, *44*, 2395. (c) Rabindranath, A. R.; Zhu, Y.; Heim, I.; Tieke, B. *Macromolecules* **2006**, *39*, 8250. (d) Zhu, Y.; Rabindranath, A. R.; Beyerlein, T.; Tieke, B. *Macromolecules* **2007**, *40*, 6981. (e) Zhang, K.; Tieke, B. *Macromolecules* **2008**, *41*, 7287. (f) Burgi, L.; Trubiez, M.; Pfeiffer, R.; Bienewald, F.; Kirner, H. J.; Winnewisser, C. *Adv. Mater*. **2008**, *20*, 2217. (g) Tantiwiwat, M.; Tamayo, A. B.; Luu, N.; Dang, X. D.; Nguyen, T. Q. *J. Phys. Chem. C* **2008**, *112*, 17402.
(7) Wallquist, O.; Lenz, R. *Macromol. Symp*. **2002**, *187*, 617.
(8) (a) Wienk, M. M.; Turbiez, M.; Gilot, J.; Janssen, R. A. J. *Adv. Mater*. **2008**, *20*, 2556. (b) Tamayo, A. B.; Tantiwiwat, M.; Walker, B.; Nguyen, T. Q. *J. Phys. Chem. C* **2008**, *112*, 15543. (c) Tamayo, A. B.; Walker, B.; Nguyen, T. Q. *J. Phys. Chem. C* **2008**, *112*, 11545. (d) Tamayo, A. B.; Dang, X. D.; Walker, B.; Seo, J.; Kent, T.; Nguyen, T. Q. *Appl. Phys. Lett*. **2009**, *94*, 103301. (e) Zhou, Y. P.; Gendron, D.; Badrou-Ach, R.; Najari, A.; Tao, Y.; Leclerc, M. *Macromolecules* **2009**, *42*, 2891.
(9) Hou, J. H.; Park, M. H.; Zhang, S. Q.; Chen, L. M.; Li, J. H.; Yang, Y. *Macromolecules* **2008**, *41*, 6012.
(10) Miura, M.; Satoh, T.; Watanabe, H.; Ueda, M. 2007, WO/2007/105638.
(11) Rochat, A. C.; Cassar, L.; Iqbal, A. US Patent 4579949, 1986.
(12) Li, Y. F.; Cao, Y.; Gao, J.; Wang, D. L.; Yu, G.; Heeger, A. J. *Synth. Met*. **1999**, *99*, 243.
(13) Kaneto, K.; Lim, W. Y.; Takashima, W.; Endo, T.; Rikukawa, M. *Jpn. J. Appl. Phys*. **2000**, *39*, L872.
(14) Nguyen, L. H.; Hoppe, H.; Erb, T.; Gunes, S.; Gobsch, G.; Sariciftci, N. S. *Adv. Funct. Mater*. **2007**, *17*, 1071.